



The Effect of the Variation of Volume Flow Rate on the Thermal Parameters of a Solar Air Collector with a Single Pass of Air: Case Study for Laghouat, Algeria

D. Bensahal*, A. Yousfi

Laboratory of Mechanic, Faculty of Technology, University of Laghouat, Algeria

PAPER INFO

Paper history:

Received 27 September 2017

Received in revised form 25 November 2017

Accepted 30 November 2017

Keywords:

Volume Flow Rate
Solar Air Collector
Temperature
Efficiency

ABSTRACT

The effect of the volume flow rate of the heat transfer fluid (air) on the thermal parameters of the solar air collector with a single air pass without using fins under the absorbing plate have been investigated experimentally and theoretically. We use a new design of solar air collector which aims to optimize these parameters in the region cited above. Our solar air collector was realized at the mechanical workshop at the University of Laghouat, Algeria. We chose five different volume flow rates for five different days. This study shows the evolution of the thermal parameters of the solar air collector as function of the local solar time (Lst) such as: absorber temperature, temperature of the bottom plate, outlet temperature, ambient temperature, solar irradiation intensity and efficiency for a tilt angle of solar collector equal 36.7°. We observe clearly that the daily efficiency and the outlet temperature of our solar air collector increase with increasing of the flow rate ($\eta = 8.72\% \sim 28.82\%$, $60^\circ\text{C} \sim 70^\circ\text{C}$) exceptly for flow rates 3 and 4 (partial sky condition). The average temperature of bottom plate, the transparent cover and absorber temperature decrease such as: ($73^\circ\text{C} \sim 64^\circ\text{C}$, $66.5^\circ\text{C} \sim 45.09^\circ\text{C}$, $128^\circ\text{C} \sim 124^\circ\text{C}$) when the volume flow rate is increasing. We observe a good agreement between the values obtained theoretically and those obtained experimentally except for the volume flow rates 3 and 4 (partial sky condition).

doi: 10.5829/ije.2018.31.01a.11

NOMENCLATURE

V_w	Wind speed (m/s)
T	Temperature (K)
T_c	Equivalent temperature of the sky (K)
L	Length of solar collector (m)
Nu	Nusselt number
k_f	Conductivity of the fluid [W / (m.K)]
D_H	Hydraulic diameter (m)
Re	Reynolds number
V_f	Fluid velocity (m/s)
\dot{m}	Mass flow (kg/s)
A_f	Fluid passage section (m ²)
U_{av}	Front loss coefficient
I	Solar irradiation intensity (W/m ²)
Q_u	The useful energy gain (W)
C_p	Specific heat of the air
A_c	The area of the collector (m ²)
l	Width of solar collector
LST	Local solar time (hour)

Greek Symbols

β	Tilt angle (solar collector - ground) (°)
ρ	Density (kg/m ³)
σ	Constant of Stephan Boltzmann [W/(m ² .k ⁴)]
ε	Emissivity
α	Absorptivity
η	Thermal efficiency
τ	Transmittance

Subscripts

h_c	Convective transfer coefficient [W/(m ² .K)]
h_r	Radiative transfer coefficient [W/(m ² .K)]
h_d	Conductive transfer coefficient [W/(m ² .K)]
p	Absorber
pl	Bottom plate
v	Transparent cover or glass
c	Sky
ab	Ambiant
f	Fluide
s	Ground
is	Insulating plate

*Corresponding Author's Email: bensahal.dz@gmail.com (D. Bensahal)

Please cite this article as: D. Bensahal, A. Yousfi, The Effect of the Variation of Volume Flow Rate on the Thermal Parameters of a Solar Air Collector with a Single Pass of Air: Case Study for Laghouat, Algeria, International Journal of Engineering (IJE), IJE TRANSACTIONS A: Basics Vol. 31, No. 1, (January 2018) 71-78

1. INTRODUCTION

Most of the solar thermal collectors used worldwide are evacuated tube collectors, since China has by far the largest solar thermal market and almost all collectors used in China are of the type evacuated tube. In contrast, about 90% of the solar collectors used in Europe are flat plate collectors. Up to now, almost all collectors use a liquid heat transfer medium, but use of air heating collector is increasing which is based on these characteristics. Which type of collector “is best” depends on the intended application, location of use, required performance and operating temperatures, the typical ambient temperature range, the type of heating system in which the collector is to be integrated, as well as on mounting and aesthetic requirements, and of course the available budget. However, the most important factor for choosing a solar collector type is the required operating temperature range. The application areas are performed by their typical temperature ranges and the related collector types with their typical outlet temperatures [1].

In solar air heaters, energy is transferred directly from a remote source of radiant energy into the air. Transmitted heat can then be used by passing air through a conduit system located between the bottom and the absorber plate. The heated air is then used to heat homes [2, 3]. Solar drying is one of the best choices in this context. The research is progressing in most of the countries to propagate the solar drying technology for value addition of agriculture products. The solar drying technology is a classical example to showcase how sun’s free energy could be effectively utilized for the benefit of mankind [4-7]. An experimental investigation has been carried out for a series of system and operating parameters in order to analyze the effect of mass flow rate on heat transfer and Nusselt number characteristics in solar air heater. Experiments are performed at different air mass flow rates; varying from 0.012 to 0.016 kg/s, about hot summer days of Mai 2012. The effects of mass flow rate of air on the outlet temperature, Nusselt Number, Reynolds Number, Prandtl Number, the heat transfer in the thickness and length of the solar air collector were studied [8, 9]. Optimal homotopy asymptotic method (OHAM) and homotopy perturbation method (HPM) are applied to investigate heat transfer in the air-heating flat-plate solar collectors. As an important outcome, increasing in the collector’s dimensions (width and length) make a decreasing in thermal efficiency, but increasing in air mass flow rates improve it [10-13].

In this work, we present a theoretical and experimental study of a solar air collector without fins. The aim of this study is to show the effect of the volume flow rate on the heat transfer fluid (air) on the thermal parameters of the air solar collector with a single air pass in the region of Laghouat, Algeria.

2. MODELING OF HEAT EXCHANGE COEFFICIENTS

The type of solar collector used for the conversion of solar energy into thermal energy in this study is presented in Figure 1.

2.1. Convective Transfer For the wind transfer, the coefficient is defined as a linear function of the wind speed (V_w : wind speed [m/s]). Several studies use the formulation below:

$$h_{c_v} = 5,67 + 3,86.V_w \quad (1)$$

Between the transparent cover and the absorber, we have through the immobile air gap existing between the transparent cover and the absorber :

$$h_{c_nat} = 1,42 \cdot \left\{ \frac{(T_p - T_{ab}) \cdot \sin(\beta)}{L} \right\}^{1/4} \quad (2)$$

The ambient temperature can be calculated according to Idliman [14].

In the mobile air, the following correlations were established by Duffie and Backman [4, 15] (without fins):

$$h_c = \frac{Nu \cdot k_f}{D_H} \quad (3)$$

It is also possible to use the following correlation which was established by Kays [16]:

$$Nu = 0,0158 \cdot Re^{0,8} \quad (4)$$

In the case of the absorbers provided with fins to pass through the Colburn, factor "J" takes into consideration the flow regime through the Reynolds, and the geometry of the fins [17]. The convective exchange between the heat transfer fluid and the absorber can be given by Equation (5):

$$h_{cp_f} = \frac{Nu \cdot k_f}{D_H} \quad (5)$$

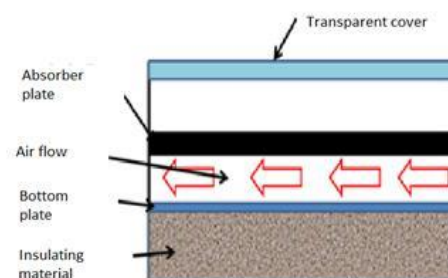


Figure 1. Schematic view of the box solar collector without fins

The convective exchange between the heat transfer fluid and the insulating plate is given by:

$$h_{cpl_f} = h_{cp_f} \quad (6)$$

The evaluation of the fluid velocity is:

$$V_f = \frac{\dot{m}}{\rho_f \cdot A_f} \quad (7)$$

2. 2. Radiant Transfer The radiative exchange between the transparent cover and the celestial vault is as follow [18]:

$$h_{rv_c} = \sigma \cdot \varepsilon_v \cdot \left(\frac{1 - \cos(\beta)}{2} \right) \cdot (T_v + T_c) \cdot (T_v^2 + T_c^2) \quad (8)$$

The equivalent temperature of the sky T_c is [19]:

$$T_c = 0,0552 \cdot T_{ab}^{3/2} \quad (9)$$

The radiative exchange between the transparent cover and the absorber is:

$$h_{rp_v} = \frac{\sigma \cdot (T_v + T_p) \cdot (T_v^2 + T_p^2)}{\frac{1}{\varepsilon_v} + \frac{1}{\varepsilon_{p_v}} - 1} \quad (10)$$

The radiative exchange between the transparent cover and the ground is:

$$h_{rv_s} = \sigma \cdot \varepsilon_v \cdot \left(\frac{1 + \cos(\beta)}{2} \right) \cdot (T_v + T_s) \cdot (T_v^2 + T_s^2) \quad (11)$$

The radiative exchange between the absorber and the bottom plate is given by Equation (12):

$$h_{rp_pl} = \frac{\sigma \cdot (T_{pl} + T_p) \cdot (T_{pl}^2 + T_p^2)}{\frac{1}{\varepsilon_{p_pl}} + \frac{1}{\varepsilon_{pl}} - 1} \quad (12)$$

The radiative exchange between the insulation and the ground is:

$$h_{ris_s} = \frac{1}{2} \cdot \sigma \varepsilon_{is} [1 + \cos(\pi - \beta)] \cdot (T_{is} + T_s) \cdot (T_{is}^2 + T_s^2) \quad (13)$$

2. 3. Front Loss Coefficients Klein proposes to calculate the coefficient of the front losses of the absorber by the following expression [20]:

$$U_{av} = h_{c-v} + h_{rv-c} \quad (14)$$

2. 4. Establishment of the Equation of Thermal Equilibrium of Solar Collector The thermal equilibrium of the transparent cover is [18]:

$$-(T_v - T_{ab}) \cdot h_{c-v} - (T_v - T_c) \cdot h_{rv-c} - (T_v - T_s) \cdot h_{rv-s} + (T_v - T_p) \cdot \left\{ \frac{h_{c_nat}}{2} + h_{rp-v} \right\} + \alpha_v \cdot I_t = 0 \quad (15)$$

The thermal equilibrium of the absorber is:

$$-(T_p - T_v) \cdot \left\{ \frac{h_{c_nat}}{2} + h_{rp-v} \right\} - (T_p - T_f) \cdot h_{cp-f} - (T_p - T_{pl}) \cdot h_{rp-pl} + \tau_v \cdot \alpha_p \cdot I_t = 0 \quad (16)$$

The thermal equilibrium of the heat transfer fluid is:

$$(T_p - T_f) \cdot h_{cp-f} - (T_f - T_{pl}) \cdot h_{cpl-f} - dQu/(l \cdot dx) = 0 \quad (17)$$

The thermal equilibrium of the bottom plate is as below:

$$(T_f - T_{pl}) \cdot h_{cpl-f} + (T_p - T_{pl}) \cdot h_{rp-pl} - (T_{pl} - T_{is}) \cdot h_d = 0 \quad (18)$$

The thermal equilibrium of the external insulating plate is given by Equation (19):

$$(T_{pl} - T_{is}) \cdot h_d - (T_{is} - T_{ab}) \cdot h_{c-v} - (T_{is} - T_s) \cdot h_{ris-s} = 0 \quad (19)$$

We have a system of 5 equations for 5 unknowns which represent the temperatures put in the form of a vector T_i (T_v , T_p , T_f , T_{pl} et T_{is}) which will be solved by the numerical method. For the resolution, the matrix form is: $[A_{ij}] [T_i] = [C_i]$.

3. EXPERIMENTS

A schematic view of the solar air collector without fins is shown in Figure 2. After the solar air collector startup air plane and letting him work for several days under normal weather conditions. Thermocouples (model:DC-M02, range of temperature displayed:-50°C ~150 °C, Accuracy: $\pm 1^\circ\text{C}$) were placed uniformly on the upper surface of the absorber plate and bottom plate at identical positions along the direction of flow.

Two other thermocouples were used to measure inlet and outlet air temperatures. The distribution of the thermocouples as follows: four thermocouples were used to measure the temperatures of absorber and the same number for the bottom plate. All temperatures were measured in degrees Celsius ($^\circ\text{C}$).

Non-contact digital infrared thermometer (model: PCE-777) is used to measure the temperature of the ground and transparent cover (Temp. Range:-30°C to 260 °C, resolution:0.1 °C, basic accuracy: $\pm 2\%$, response time: less than 1 second). The solar radiation incident on the collector surface was measured with a Solarimeter (model: Kimo SL200)(Solar irrigation measuring range:1 W/m² to 1300 W/m², operating temperature: -10°C to +50°C, accuracy:5% of measurement, frequency of the measure: 2/s).

This solar collector was oriented towards the south. The measured variables were recorded at a time interval of 30 minutes and included: irradiation, inlet and outlet air temperatures of the fluid circulating in the solar collector, ambient temperature, and temperatures of the absorber surface at several selected locations.

The air flows were measured by a digital anemometer (model: Lutron AM-206M, measurement air velocity : operating 0°C to 50°C, range: 0.4-35.0 m/s, resolution:0.1 m/s, accuracy:± (2 % + 0.2 m/s). All tests started at 9 am and ended at 4 pm.

Table 1 shows the experimental conditions: angle, volume flow rate used, time of day and condition of the sky. The dimension of the main components of the solar air collector: length, width and thickness are shown in Table 2. The thermo-physical characteristics of the different constituents are shown in Table 3.



Figure 2. The photograph of experimental set-up

TABLE 1. The experimental conditions: angle, flow rate, time of day and condition of the sky.

N°	Angle of inclination (°)	Flow rate (m ³ / s)	Date of the day	Sky conditions
1	36.7	0.0041475	13.03.2017	clear
2	36.7	0.00819546	09.03.2017	clear
3	36.7	0.01002036	05.02.2017	partial
4	36.7	0.01118166	06.03.2017	partial
5	36.7	0.0129402	03.03.2017	clear

TABLE 2. The dimension of the components of the solar air collector

Component	Length (m)	Width (m)	Thickness (mm)
Transparent cover	1.94	0.94	4
Absorber	1.94	0.94	1
Bottom plate	1.94	0.94	1
Insulation	1.94	0.94	40
Wood Case	2	1	80

TABLE 3. Thermo-physical characteristics of the different constituents

Component	Materials	density (kg/m ³)	Specific heat (J/kg.°K)	Thermal conductivity (W/m.°K)
Transparent cover	Plexiglass	1.2	1500	1.5
Absorber, bottom plate	Galvanized iron	7800	473	45
Insulation	Expanded polystyrene	16	1670	0.037

4. RESULTS AND DISCUSSIONS

In the present work, we present all the results obtained experimentally collected by our thermocouples and infrared sensors and we try to make comparisons between the experimental and the theoretical results in order to see the effect of variation of air flow rate on parameters studied. All the temperatures of different elements increase with local solar time (LST) as solar radiation shows their maximum values at 13h:30.

4. 1. Absorber Temperature It can be seen from Figures 3 and 4, that the curves of temperature of absorber tend to decrease with increasing air flow rate. These results show that for a good heating of the absorber, it will be always necessary to proceed with a lower air flow rate as shown in Figures 4 and 5.

For flow rate 1, the maximum temperature of the absorber reaches 128 °C, for flow rate 2, it reaches 125 °C and finally for flow rate 5, it reaches 124 °C at 13h:30 (LST). When the air flow rate increases, we observe a decrease in temperature for the absorber, that is significant a slight cooling of the absorber as shown in Figure 5.

4. 2. Bottom Plate Temperature Regarding the temperature of the bottom plate at 14h, there is a decrease in the average temperature gradually as the flow rate increases.

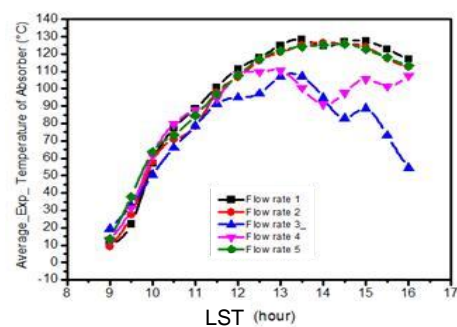


Figure 3. Comparison of experimental average temperatures of the absorber as function of LST for the five flow rates studied

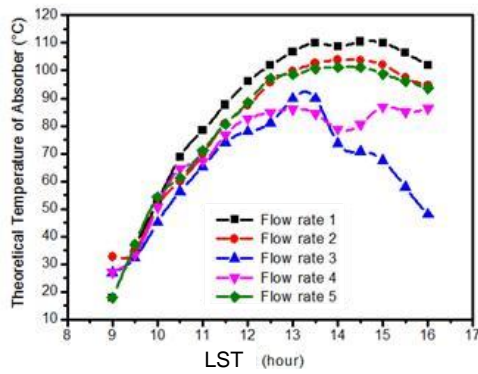


Figure 4. Comparison of the theoretical temperatures of the absorber as function of time LST for the five flow rates studied

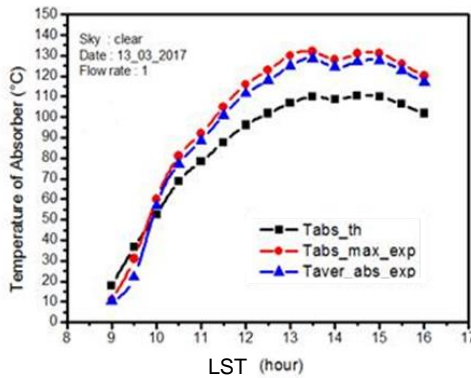


Figure 5. Comparison between the theoretical, maximum and average temperature of the absorber obtained experimentally as function of LST with flow rate 1

For the flow rate 1, 2 and 5, the average temperature reaches 73 °C, 67 °C and 64 °C. It can be concluded that the temperature of the bottom plate has the same acts as the absorber. It recognizes a decrease in temperature when the flow rate increases as shown in Figure 6. The Figure 7 shows clearly the effect of flow rate on the temperature of the bottom plate. It recognizes a decrease in temperature when the flow rate increases.

4. 3. Outlet Temperature The Figure 8 presents an increase in the output temperature when the local solar time increases. The theoretical curve has a difference of 25 °C, 7 °C and 0.66 °C compared to the experimental curve at 13h: 30 for the flow rate: 1, 2 and 5.

A comparison between experimental outlet temperature is established for different flow rates depending on the local solar time (LST) and shown that when the flow rate increases, the outlet temperature of the solar collector also increases except for the flow rates of 3 and 4 (partial sky condition) as shown in Figure 9.

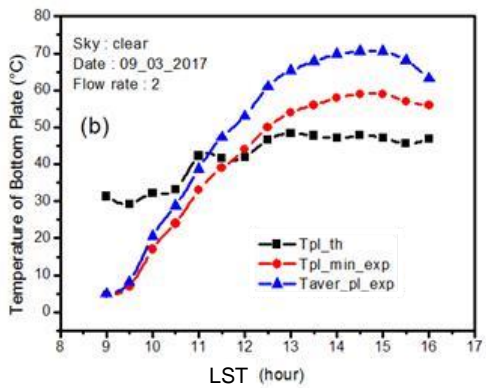
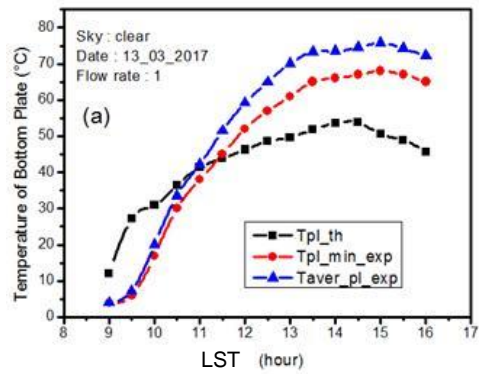


Figure 6. Comparison between the theoretical, minimum and average temperature of the bottom plate obtained experimentally as a function of LST with volume flow rates: (a) 1, and (b) 2

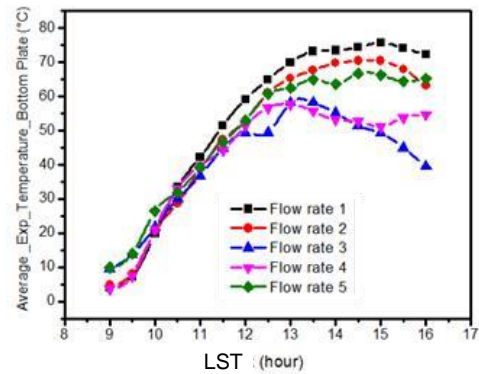


Figure 7. Comparison of average experimental temperatures of the bottom plate as function of LST for the five flows rates studied

4. 4. Transparent Cover Temperature For the flow rate 1, the maximum temperature of the transparent cover reaches 66.5 °C, for the flow rate 2, it reaches 48.06 °C and finally for the flow rate 5, it reaches 45.09 °C at 13h30 (LST) as shown in Figure 10.

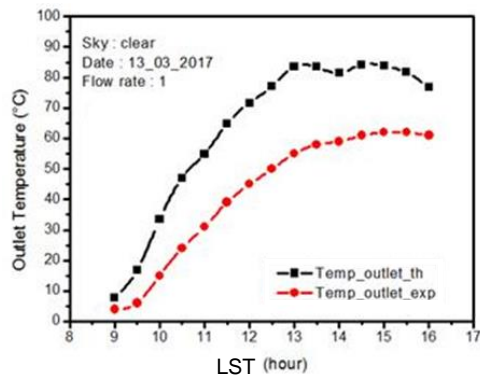


Figure 8. Comparison between the theoretical and experimental outlet temperature as function of LST with volume flow rate 1

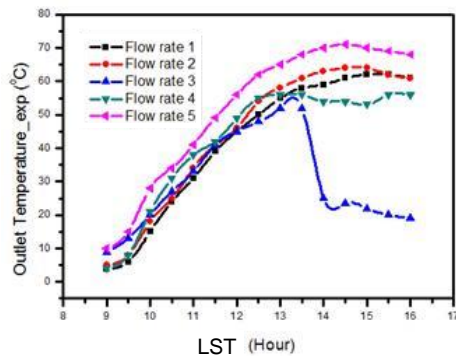


Figure 9. Comparison of experimental outlet temperatures as function of LST for the five flow rates studied

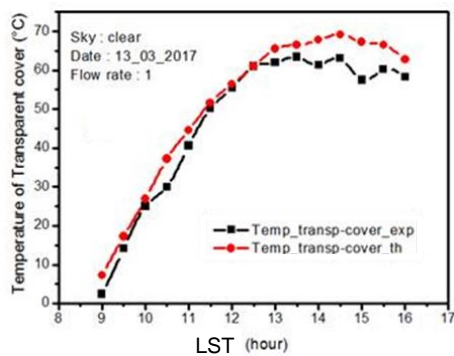


Figure 10. Comparison between the theoretical and experimental temperature of transparent cover as function of LST with volume flow rate 1

A comparison between theoretical temperature is established for different flow rates depending on the local solar time (LST) and shown that when the flow rate increases, the temperature of the transparent cover of the solar collector also decreases except for the flow rate 3 (partial sky condition) as shown in Figure 11.

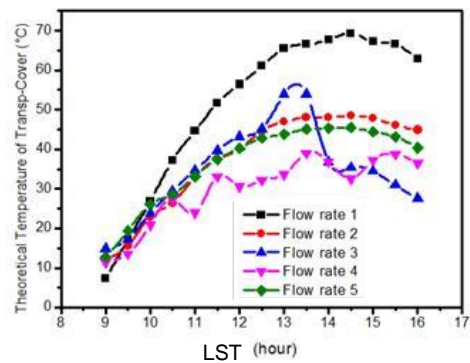


Figure 11. Comparison of theoretical temperatures of transparent cover as function of LST for the five flow rates studied

4. 5. Ambient Temperature The Figure 12 shows a good agreement between the values obtained theoretically and those obtained experimentally of the ambient temperature. We present only the ambient temperature for flow rate1.

4. 6. Solar Irradiation We present in Figure 13 the variation of solar irradiation as function of the time of the day for the five days studied in the region of Laghouat, Algeria. We observe an increasing in intensity of solar irradiation until at noon 13h30 (LST) (maximum value) exceptly for the two days representing the flow rates 3 and 4 (presence of clouds in sky). After that, the solar intensity decreases respectively.

4. 7. Thermal Efficiency (η) The efficiency (%) of solar collector is given by the following equation [21]:

$$\eta = m \cdot Cp \cdot \frac{(T_{out} - T_{in})}{I \cdot Ac} \quad (21)$$

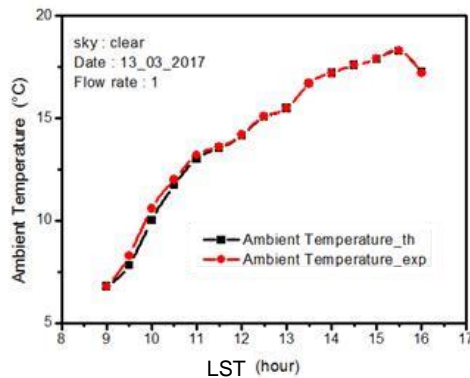


Figure 12. Comparison between the theoretical and experimental ambient temperature as a function of LST with flow rate 1

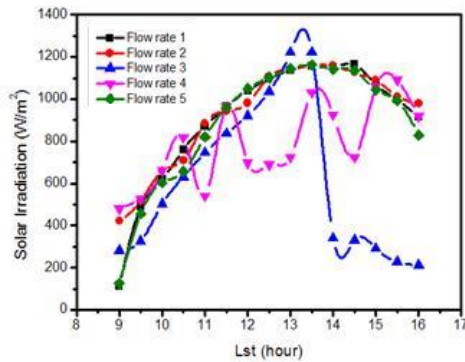


Figure 13. Hourly variation of the solar irradiation for five flow rates studied as function of LST

where:

The masse flow rate is:

$$\dot{m} = \rho \cdot V \quad (22)$$

The specific heat of air is:

$$C_p = 999.23 + 0.1434 T_f + 1.101.10^{-4} T_f^2 - 6.7581.10^{-8} T_f^3 \quad (23)$$

The density of air is given by the following Equation:

$$\rho = 1.204 \left(\frac{293}{T_f} \right) \quad (24)$$

We observe clearly that the daily efficiency of our solar air collector increases with increasing of the flow rate exceptly for flow rates 3 and 4 (partial sky condition) as shown in Figure 14.

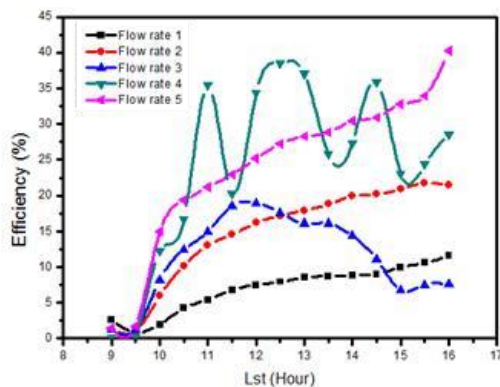


Figure 14. Effect of the volume flow rate on the daily efficiency of the solar collection in the region of Laghouat, Algeria

The values of the efficiency at noon (13h30) are: $\eta = 8.72\%$ for volume flow rate 1, $\eta = 18.83\%$ for volume flow rate 2, $\eta = 16.12\%$ for volume flow rate 3, $\eta = 25.76\%$ for volume flow rate 4, $\eta = 28.82\%$ for volume flow rate 5.

5. CONCLUSIONS

In this work, we studied the effect of the volume flow rate variation on the behavior of our solar air collector with a single air pass. The mathematical formulation of the problem studied is taken from the literature. We used Matlab software to develop a program that takes into account the energy balance of our solar air collector that will be object of comparison later with experimental results. For the absorber temperature, when the flow rate increases, we observe a decrease in temperature for the absorber which implies a cooling of the absorber. For the temperature of the bottom plate, we observe the same acts as the absorber. It recognizes a decrease in temperature when the flow rate increases too. For the ambient temperature, we observe a good agreement between the values obtained theoretically and those obtained experimentally. When the flow rate increases, the outlet temperature of the solar collector also increases except for the flow rate 3 and 4 (partial sky condition). The same considerations mentioned for the outlet temperature are also valid for the transparent cover temperature obtained experimentally. The thermal efficiency increases with increasing volume flow rate exceptly for flow rates 3 and 4 (partial sky condition). In addition, the intensity of solar irradiation depends on the weather conditions.

6. REFERENCES

1. Richter, C., Lincot, D. and Gueymard, C.A., "Solar energy, New York, Springer, (2013).
2. Garg, H. and Adhikari, R., "Performance evaluation of a single solar air heater with n-subcollectors connected in different combinations", *International Journal of Energy Research*, Vol. 23, No. 5, (1999), 403-414.
3. Belusko, M., Saman, W. and Bruno, F., "Performance of jet impingement in unglazed air collectors", *Solar Energy*, Vol. 82, No. 5, (2008), 389-398.
4. Duffie, J.A. and Beckman, W.A., "Solar engineering of thermal processes", New York, 2th Edn. Wiley, (1980).
5. Koyuncu, T., "Performance of various design of solar air heaters for crop drying applications", *Renewable Energy*, Vol. 31, No. 7, (2006), 1073-1088.
6. Ratti, C. and Mujumdar, A., "Solar drying of foods: Modeling and numerical simulation", *Solar Energy*, Vol. 60, No. 3-4, (1997), 151-157.
7. Khamforoush, M., Mirfatah, S. and Hatami, T., "Application of three types of dryers namely tunnel, fluidized bed, and fluidized bed with microwave for drying of celery, corn, and sour cherry: Experiments and modeling", *International Journal of*

- Engineering-Transactions B: Applications*, Vol. 27, No. 5, (2014), 667.
8. Yeh, H.-M. and Lin, T.-T., "The effect of collector aspect ratio on the collector efficiency of flat-plate solar air heaters", *Energy*, Vol. 20, No. 10, (1995), 1041-1047.
 9. Chabane, F., Moumimi, N., Bensahal, D. and Brima, A., "Heat transfer coefficient and thermal losses of solar collector and nusselt number correlation for rectangular solar air heater duct with longitudinal fins hold under the absorber plate", *Applied Solar Energy*, Vol. 50, No. 1, (2014), 19-26.
 10. Ghasemi, S., Hatami, M. and Ganji, D., "Analytical thermal analysis of air-heating solar collectors", *Journal of Mechanical Science and Technology*, Vol. 27, No. 11, (2013), 3525-3530.
 11. Karim, M.A. and Hawlader, M., "Performance investigation of flat plate, v-corrugated and finned air collectors", *Energy*, Vol. 31, No. 4, (2006), 452-470.
 12. Nowzari, R., Aldabbagh, L. and Egelioglu, F., "Single and double pass solar air heaters with partially perforated cover and packed mesh", *Energy*, Vol. 73, (2014), 694-702.
 13. Kumar, S. and Saini, R., "Cfd based performance analysis of a solar air heater duct provided with artificial roughness", *Renewable Energy*, Vol. 34, No. 5, (2009), 1285-1291.
 14. Idlimam, A., "Etude théorique d'un système de séchage des peaux et des cuirs pour la région de marrakech constitué d'une serre agricole jouant le rôle de générateur solaire d'air chaud et d'un séchoir conventionnel", *These de 3eme cycle, Ecole Normale Supérieure, Marrakech, Maroc*, (1990).
 15. Ajay, K. and Kundan, L., "Performance evaluation of nanofluid (al₂o₃/h₂o-c₂h₆o₂) based parabolic solar collector using both experimental and cfd techniques", *International Journal of Engineering-Transactions A: Basics*, Vol. 29, No. 4, (2016), 572.
 16. Kays, W.M., "Convective heat and mass transfer, Tata McGraw-Hill Education, (2012).
 17. Youcef-Ali, S. and Desmons, J., "Simulation of a new concept of an indirect solar dryer equipped with offset rectangular plate fin absorber-plate", *International journal of energy research*, Vol. 29, No. 4, (2005), 317-334.
 18. Chabane, F., "Modélisation des paramètres de la conversion thermique de l'énergie solaire", Université Mohamed Khider-Biskra, *Applied Solar Energy*, Vol. 50, No. 1, (2014), 19-26.
 19. Kasaeian, A., Mobarakeh, M.D., Golzari, S. and Akhlaghi, M., "Energy and exergy analysis of air PV/T collector of forced convection with and without glass cover", *International Journal of Engineering-Transactions B: Applications*, Vol. 26, No. 8, (2013), 913.
 20. Klein, S. and Beckman, W., "A general design method for closed-loop solar energy systems", *Solar Energy*, Vol. 22, No. 3, (1979), 269-282.
 21. Goudarzi, K., Asadi, Y.A.S., Shojaeizadeh, E. and Hajipour, A., "Experimental investigation of thermal performance in an advanced solar collector with helical tube", *International Journal of Engineering, Transaction A: Basics*, Vol. 27, No. 7, (2014), 1149-1154

The Effect of the Variation of Volume Flow Rate on the Thermal Parameters of a Solar Air Collector with a Single Pass of Air: Case Study for Laghouat, Algeria

D. Bensahal, A. Yousfi

Laboratory of Mechanic, Faculty of Technology, University of Laghouat, Algeria

PAPER INFO

چکیده

Paper history:

Received 27 September 2017

Received in revised form 25 November 2017

Accepted 30 November 2017

Keywords:

Volume Flow Rate
Solar Air Collector
Temperature
Efficiency

تأثیر نرخ جریان حجمی سیال انتقال حرارتی (هوا) بر پارامترهای حرارتی کلکتور هوای خورشیدی با عبور هوا بدون استفاده از فین ها تحت ورقه جذب شده به صورت تجربی و نظری مورد بررسی قرار گرفته است. ما از یک طراحی جدید از کلکتور هوای خورشیدی استفاده می کنیم که هدف آن بهینه سازی این پارامترها در منطقه ذکر شده بالا است. کلکتور خورشیدی ما در کارگاه مکانیکی در دانشگاه لاگووات الجزایر تحقق یافت. ما پنج حجم مختلف جریان حجمی را برای پنج روز انتخاب کردیم. این مطالعه نشان می دهد که تکامل پارامترهای حرارتی کلکتور خورشیدی به عنوان تابعی از زمان خورشیدی محلی (LST)، از قبیل: دمای جذب شده، دمای صفحه پایین، دمای خروجی، دمای محیط، شدت تابش خورشیدی و کارایی برای یک شیب زاویه کلکتور خورشیدی برابر با ۳۶/۷ درجه است. ما به وضوح مشاهده می کنیم که بهره وری روزانه و دمای خروجی کلکتور خورشیدی ما با افزایش سرعت جریان $\eta = 8.72\% \sim 28.82\%$ در 60°C شفاف و دمای جذب شده مانند: $(70^\circ\text{C}$ ، به استثنای سرعت جریان ۳ و ۴ (شرایط آسمان جزئی) افزایش می یابد. دمای متوسط صفحات پایینی، پوشش $73^\circ\text{C} \sim 64^\circ\text{C}$ ، $66.5^\circ\text{C} \sim 45.09^\circ\text{C}$ ، $128^\circ\text{C} \sim 124^\circ\text{C}$) کاهش می یابد هنگامی که نرخ جریان حجمی در حال افزایش است. ما توافق خوبی را بین مقادیر به دست آمده به صورت تئوری آزمایشگاهی، به جز نرخ جریان های حجمی ۳ و ۴ (شرایط آسمان جزئی) مشاهده می کنیم.

doi: 10.5829/ije.2018.31.01a.11